

Ab initio study of the migration of small polarons in olivine Li_xFePO_4 and their association with lithium ions and vacancies

Thomas Maxisch,^{1,*} Fei Zhou,² and Gerbrand Ceder^{1,†}

¹*Department of Materials Science and Engineering, Massachusetts Institute of Technology, Cambridge, Massachusetts 02139, USA*

²*Department of Physics, Massachusetts Institute of Technology, Cambridge, Massachusetts 02139, USA*

(Received 24 October 2005; revised manuscript received 23 January 2006; published 13 March 2006)

Using first-principles pseudopotential calculations, we investigate the formation and transport of small polarons in olivine Li_xFePO_4 . It is demonstrated that excess charge carriers form small polarons in LiFePO_4 and FePO_4 . Lower limits to the activation barrier for small polaron migration are calculated within the GGA+U framework. Additionally, the interaction between lithium ions and polarons is investigated and estimates of binding energies between lithium ions and polarons are provided. Our results show that the binding energy between electron polarons and Li^+ ions in FePO_4 is lower than that between hole polarons and lithium vacancies in LiFePO_4 . The electron transfer rate is predicted to be higher in FePO_4 than in LiFePO_4 .

DOI: [10.1103/PhysRevB.73.104301](https://doi.org/10.1103/PhysRevB.73.104301)

PACS number(s): 71.38.Ht, 82.47.Aa, 72.20.-i, 71.15.Mb

I. INTRODUCTION

Layered Li_xMPO_4 ($M=\text{Fe}, \text{Mn}, \text{Co}, \text{Ni}$) olivine phosphate materials are of interest as possible cathode material in rechargeable Li-ion batteries. In this family of compounds, Li_xFePO_4 has thus far shown the most promise.^{1,2} It has a theoretical capacity of 170 mA h/g, combined with a lithium intercalation potential of 3.5 V,³ and exhibits an excellent thermal stability. In addition, it has the potential to be inexpensive, making it of interest for large scale battery applications. However, in their pure form, olivine phosphates suffer from a low intrinsic electron conductivity in the range from 10^{-10} S/cm to 10^{-5} S/cm, limiting their rate capability and, hence, their device applicability.^{4,5} Nevertheless, efforts to improve the conductivity by carbon coating, control of grain size, and the creation of conducting networks lead to a significant increase of the rate capability.^{3,6} However, these approaches do not address the intrinsic conductivity of the cathode material itself. In order to determine the limiting factors for charge transport in these compounds, a better understanding of the lithium ion and electron mobility is needed.

A recent investigation on Li^+ diffusion in olivine phosphates predicts a high intrinsic ionic mobility through one-dimensional channels.⁷ Experimental values for the activation energy to electronic conductivity of pristine LiFePO_4 are spread over a wide range and depend highly on the experimental setup. Takahashi *et al.*⁸ and Shi *et al.*⁹ report low values of 156 meV and 186 meV, respectively, while others indicate substantially higher values between 390 meV and 630 meV.^{4,5,10} A significant controversy exists about the origin of the low intrinsic electron conductivity and whether it can be improved by doping, indicating that the conduction mechanism is not yet fully understood.^{4,6,11,12} The aim of the present work is to address the intrinsic electron conductivity in Li_xFePO_4 by means of *ab initio* calculations and to illustrate that the electron transport mechanism can be understood by means of diffusion of small polarons.

II. SMALL POLARON MIGRATION

A vast body of literature on electron transfer models exists and solely a brief introduction to the most fundamental

concept of small polaron transfer is provided. Greater detail is given in the reviews by Marcus,¹³ Mikkelsen and Ratner,¹⁴ Sutin,¹⁵ and Dogonadze *et al.*,¹⁶ as well as monographs by Cannon¹⁷ and Alexandrov and Mott.¹⁸

When excess charge carriers, such as electrons or holes are present in a polar crystal, the atoms in its environment are polarized and displaced producing a local lattice distortion. The ion displacement becomes more pronounced the more the charge carrier is localized. The carrier lowers its energy by localizing into such a lattice deformation and becomes self-trapped. The quasiparticle formed by the electron and its self-induced distortion is called a *small* polaron if the range of the lattice distortion is of the order of the lattice constant. In transition metal oxides, it is generally accepted that charge carriers create small polarons.^{19,20} These charge carriers can be either holes or electrons in the Li_xFePO_4 system. Lithium removal from LiFePO_4 leads to a two-phase coexistence of $\text{Li}_{1-x}\text{FePO}_4$ and Li_yFePO_4 , where x and y are believed to be rather small.^{1,21-24} Hence, the excess charge carriers are Fe^{3+} hole states in $\text{Li}_{1-x}\text{FePO}_4$ and Fe^{2+} electron states in Li_yFePO_4 , respectively. In the following, we refer to the first one as a hole polaron and to the latter one as an electron polaron.

One of the fundamental concepts of polaron hopping is that the electronic carrier cannot transfer unless a certain amount of distortion is transferred. Hence, the ionic positions are the relevant coordinates in which to describe polaron transfer. Let q contain the set of all ion coordinates in the system. In the case of an excess charge carrier localized at an iron site A , the corresponding relaxed ion coordinates are represented by q_A . At this particular point, the total energy exhibits a local minimum. The transfer of a single electron in FePO_4 between a pair of two adjacent Fe atoms, Fe_A and Fe_B , occurs by hopping between two equilibrium configurations: $\text{Fe}_A^{2+}\text{Fe}_B^{3+}$ and $\text{Fe}_A^{3+}\text{Fe}_B^{2+}$. The corresponding equilibrium configurational coordinates are labeled as q_A and q_B , respectively. In a stoichiometric FePO_4 crystal without defects or disorder, all iron crystal sites are energetically equivalent by symmetry and the total energy of the two configurations at q_A and q_B coincide. Polaron migration can be described by

the distortion of the lattice deformation along a one-dimensional trajectory on the Born-Oppenheimer surface. On a migration path from q_A to q_B , a configuration q_C exists where the total energy reaches a maximum value defining an activated state. At this transition state, the electron migrates from site A to site B transforming the system from the equilibrium state q_A to q_B . The difference between the total energy at the activated state at q_C and the initial state at q_A defines the activation energy

$$E_a = E(q_C) - E(q_A). \quad (1)$$

In contrast to the model described above, most computational studies on small polaron transfer^{25–28} employ the empirical Marcus model,^{13,29} where two independent Born-Oppenheimer surfaces around each equilibrium site are modeled under the constraint that the excess electron is either on site A or B . Marcus theory describes the electron transfer as a tunneling from one energy surface to another. The essential parameters connecting the two energy surfaces are the reorganization energy and the electron coupling between the two Born-Oppenheimer surfaces. Both values are difficult to obtain in a solid. Furthermore, these studies are typically implemented using localized basis sets for the wave functions, which limits their applicability to solids.

The approach used in this study employs a plane wave basis set allowing the continuous calculation of the total energy along the entire small polaron migration path including the transition state. Thus, no empirical models or approximations to the potential energy surface are needed. The activation energy of the polaron migration is directly accessible by calculating the energies $E(q_C)$ and $E(q_A)$. Furthermore, the plane wave framework allows us to embed small polaron migration into systems containing several hundred atoms allowing also the study of polaron-polaron and ion-polaron interactions. Our approach is “adiabatic,” assuming that when the system can change its ionic configuration to lower its energy by crossing the activated state at q_C it also does so, that is no limitations from the electron tunneling rate are present.

III. METHODOLOGY

The local density approximation (LDA) and the generalized gradient approximation (GGA) to density functional theory have proven to be very powerful methods to study the ground state electronic and magnetic structure of metals and most semiconductors. They have, however, been less successful in describing transition metal oxides, where they often inaccurately predict ground state properties, such as phase stability, magnetic, and electronic structure. Several studies investigating Li_xFePO_4 using LDA or GGA, respectively, have reported a small or even vanishing gap at the Fermi level,^{9,10,30–33} which contradicts the experimental measurements indicating a gap of approximately 3.8–4.0 eV.³⁴ In addition, excess charge carriers tend to delocalize when LDA or GGA is used, preventing any attempt to study polaron transfer.

The LDA+ U and GGA+ U methods take into account orbital dependence of the Coulomb and exchange interac-

tions which is absent in the LDA and GGA.³⁵ It has been shown that LDA+ U and GGA+ U are able to significantly improve predictions of phase stability and thermodynamic properties as well as magnetic and electronic structure in oxides.^{21,34,36–39} Quantitative results in the GGA+ U method are known to be dependent on the value of U . Since the value of U depends on the valence state of the transition metal ion,^{36,40} calculations on supercells containing both Fe^{2+} and Fe^{3+} together present a unique challenge. If not stated otherwise, in all calculations, specific values for $U=5.3$ eV and $J=1$ eV are used and taken as an averaged effective U value of $U_{\text{eff}}=(U-J)=4.3$ eV, based on self-consistently calculated U values for stoichiometric LiFePO_4 ($U_{\text{eff}}=3.7$ eV) and FePO_4 ($U_{\text{eff}}=4.9$ eV).^{36,40} The rotationally independent implementation, according to Ref. 41, which considers U and J as independent parameters has been used for this study. Using an alternative LDA+ U implementation⁴² gave activation barriers that were only a few millielectron volts different. In the following, the effective U_{eff} parameter will simply be referred to as U .

Calculations in this work are performed in a plane wave basis set using the projector augmented wave (PAW) method in the generalized gradient approximation⁴³ (GGA) as it is implemented in the VASP program.⁴⁴ Energy cutoff and k -point mesh are chosen appropriately in order to ensure the total ground state energy to be converged within 3 meV per formula unit. Internal coordinates and cell parameters of orthorhombic FePO_4 and LiFePO_4 are fully relaxed. The resulting lattice constants are $a=9.97$ Å, $b=5.91$ Å, and $c=4.86$ Å for FePO_4 , and $a=10.45$ Å, $b=6.06$ Å, and $c=4.75$ Å for LiFePO_4 . All Fe ions in FePO_4 and LiFePO_4 exhibit a high spin $t_{2g}^3(\uparrow)e_g^2(\uparrow)$ and $t_{2g}^3(\downarrow)t_{2g}^3(\uparrow)e_g^2(\uparrow)$ configuration, respectively.

Fe ions in olivine Li_xFePO_4 Fe atoms are sixfold coordinated by oxygen atoms forming layers of edge-sharing octahedra. Individual layers are separated by PO_4 tetrahedra. Thus, it is expected that electron transfer is confined to one layer and no interlayer transport occurs. If not stated otherwise, activation barrier calculations are performed using supercells containing 16 formula units in order to reduce interactions between either Li ions or polaron images. These cells are constructed by a $1 \times 2 \times 2$ replication of the olivine unit cell and incorporate two iron layers. By comparing the activation barriers to those obtained with a supercell containing 64 formula units ($1 \times 4 \times 4$), we estimate the activation barriers to be converged with respect to system size within 5 meV.

For an electron migrating from a Fe^{2+} to a neighboring Fe^{3+} site, spin conservation and the Franck-Condon principle require the alignment of the majority spin direction at both sites as prerequisites for electron transfer.⁴⁵ Hence, our calculations are performed using an A -type antiferromagnetic structure⁴⁶ in which Fe atoms within the same layer have aligned spins. Although this structure is not the magnetic ground state at zero temperature,^{21,34,36,37} we do not expect large differences with the activation energy at higher temperatures since the Néel temperatures are approximately 52 K and 125 K for LiFePO_4 and FePO_4 ,⁴⁷ respectively. Therefore, magnetic disorder with fluctuating spin directions

can be assumed at room temperature. The probability of spin alignment between two adjacent Fe sites affects the transfer probability, but not the thermal activation energy necessary to reach the transition state ionic configuration at q_C . Hence, paramagnetism may significantly lower the rate of electron transfer but does not increase its activation barrier.

The migration barrier of free polarons in stoichiometric LiFePO_4 (FePO_4), that is the fully discharged (charged) state of an Li_xFePO_4 -based rechargeable battery, is calculated by adding (removing) one extra electron to (from) the electron density. Charge neutrality of the supercell is ensured by a compensating homogeneous background charge. In order to determine the migration path, the two equilibrium end points q_A and q_B are calculated independently by a full relaxation of internal ionic coordinates. The migration path is then linearized between q_A and q_B . It is possible that there are other transition state configurations q which are not on this path, though it is unlikely that they would have significantly lower energy than the one on the linearized path. Since configurations other than the two equilibrium states at q_A and q_B , respectively, would relax to either q_A or q_B , the electron density alone is relaxed self-consistently and atom positions remain fixed for calculations along the migration path.

Additionally, it is of substantial interest whether the presence of lithium ions and vacancies, respectively, affects the activation barrier to polaron migration. In order to investigate this aspect, we also perform calculations in which a single lithium ion is removed from (added to) LiFePO_4 (FePO_4) and the total energy is calculated for a polaron migrating from an Fe site in the nearest proximity of the lithium vacancy (ion) to an Fe site as far away as possible from the vacancy (ion). In calculations investigating association energies of polarons and Li^+ ions, no electrons are added to or removed from to the charge density since the excess charge carrier is provided by the ionized lithium atoms.

IV. RESULTS

In order to investigate the migration barrier of small polarons in stoichiometric FePO_4 and LiFePO_4 without the presence of Li^+ ions or vacancies, one supplemental electron (hole) is added to the supercell of a neutral FePO_4 (LiFePO_4) crystal. The relaxed internal ion coordinates show the formation of a small polaron. The atomic on-site occupancy matrix confirms the transformation of one iron site from the $\text{Fe}^{3+}(t_{2g}^3 e_g^2)$ into the $\text{Fe}^{2+}(t_{2g}^4 e_g^2)$ configuration. The extra electron occupies a t_{2g} orbital with minority spin orientation, as it can be seen in Fig. 1, showing the isosurface of the positive part of the differential charge density, $\rho_{+1}(\mathbf{r}) - \rho_0(\mathbf{r})$, where $\rho_{+1}(\mathbf{r})$ corresponds to charge density of the supercell with the polaron and $\rho_0(\mathbf{r})$ to the charge density without the injected excess electron. Both densities are computed using the same ionic coordinates taken from the relaxed crystal with the polaron formed. The polarization of the surrounding oxygen ions induced by the polaron is also visible. The average Fe-O bond length around the Fe^{2+} site is increased to 2.15 Å compared to 2.06 Å at the surrounding Fe^{3+} sites. Similarly, a small hole polaron is formed when one electron is removed from the supercell of LiFePO_4 . In this case, one

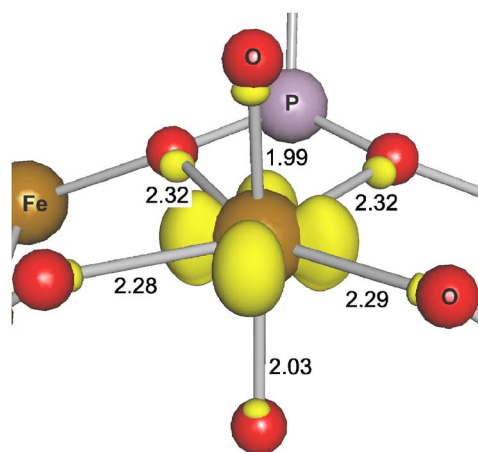


FIG. 1. (Color online) Isosurface of the charge density difference between neutral FePO_4 and a calculation with one added electron. The plotted level corresponds to $9 \times 10^{-5} e \text{ \AA}^{-3}$. The indicated bond lengths are given in angstroms.

Fe ion is transformed from $\text{Fe}^{2+}(t_{2g}^4 e_g^2)$ to $\text{Fe}^{3+}(t_{2g}^3 e_g^2)$ and the average Fe-O bond length is reduced from 2.18 Å at Fe^{2+} sites to 2.07 Å at the Fe^{3+} site.

With the ability to form polarons and to compute the equilibrium configurations q_A and q_B of two adjacent iron sites carrying a polaron, respectively, it is possible to perform static self-consistent calculations along the polaron migration path. The corresponding total energies for both hole polarons in LiFePO_4 and electron polarons in FePO_4 are shown in Fig. 2. The difference of the maximal values of the total energy at the transition state configuration q_C and the equilibrium values at q_A or q_B leads to activation energies of 215 meV for LiFePO_4 and 175 meV for FePO_4 , respectively. Thus, it is expected that *free* electron polarons migrate with a higher transfer rate in FePO_4 than *free* hole polarons in LiFePO_4 .

In order to investigate the effect of the U parameter on the activation barrier, Fig. 3(a) shows the barrier height as a function of U . Several regimes can be observed: for U values smaller than 3 eV, all Fe ions in the cell have an identical, fractional valence state and no small polaron is formed. In particular, this result demonstrates that small polarons cannot be studied in a LDA or GGA framework, which corresponds to $U=0$, as self-interaction causes the excess electron to delocalize over the entire supercell.

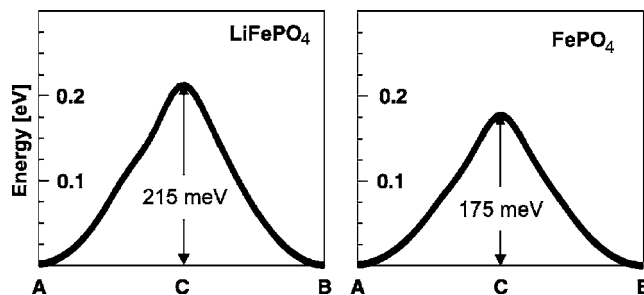


FIG. 2. Total energy along polaron migration paths between two adjacent iron sites Fe_A and Fe_B in LiFePO_4 (right panel) and FePO_4 (left panel). A, B, and C indicate the configurational coordinates q_A , q_B , and q_C , respectively.

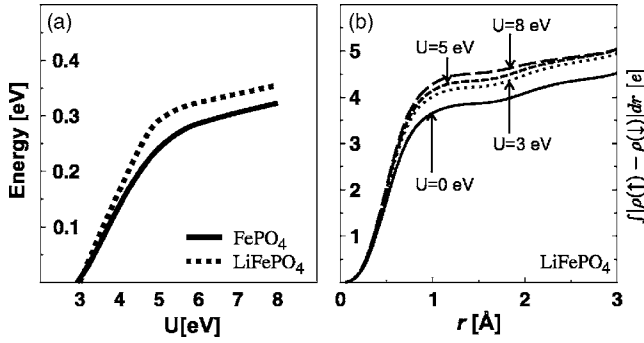


FIG. 3. Panel (a): Activation barriers to free small polaron motion in Li_xFePO_4 as a function of U . For values of U smaller than 3 eV, no small polaron formation occur. Panel (b): Integrated differential spin density at the polaron site in LiFePO_4 for several values of U as a function of integration radius.

For U values of 3 eV and larger, small polarons form and, between 3 and 5 eV, the activation barrier increases linearly as the value of U becomes larger. For U values larger than 6 eV, the activation barrier also depends linearly on the U value but with a smaller slope. The activation barrier is always higher in LiFePO_4 than in FePO_4 . One can understand the dependence of the activation barrier on the value of U by examining the spin density around the ion. An increasing value of U amplifies the localization of the d orbitals as can be learned from Fig. 3(b), which shows the integrated polarization density of a hole polaron in LiFePO_4 for different values of U . The integrated polarization density $\delta(r)$, which is defined as $\delta(r) = \int_0^r |\rho(\uparrow, r') - \rho(\downarrow, r')| dr'$ is shown as a function of sphere radius r . The average Fe-O bond length \tilde{r} around the polaron site is 2.07 Å. Value of δ of 5 and 4 electrons correspond to Fe^{3+} and Fe^{2+} ions, respectively.

For $U=0$ eV, $\delta(r)$ reaches the value of 4 electrons at \tilde{r} which indicates a Fe^{2+} ion with a $t_{2g}(\downarrow)t_{2g}^3(\uparrow)e_g^2(\uparrow)$ configuration confirming that no small polaron is formed for U values smaller than 3 eV. At $U=3$ eV, the minimum U value necessary to form a small polaron, $\delta(\tilde{r})$ is significantly higher than that obtained for $U=0$, indicating the change of the Fe ion to a $t_{2g}^3(\uparrow)e_g^2(\uparrow)$ valence state. For higher U values, $\delta(r)$ increases further. However, for values of U larger than 6 eV, $\delta(r)$ does not increase any further for radii larger than \tilde{r} , indicating the complete localization of the $t_{2g}(\downarrow)$ orbital within the oxygen octahedron which surrounds the polaron site. As a conclusion, the different slopes in Fig. 3(a) can be explained by the degree of localization of the polaron: for U values between 3 and 6 eV, the wave function of the excess charge carrier extends beyond the oxygen octahedron, allowing $t_{2g}(\downarrow)$ orbitals of adjacent Fe sites to overlap. For larger values of U , wave functions of excess charges are completely localized around the Fe site and no wave function overlap occurs resulting in higher activation energies.

In $\text{Li}_{1-x}\text{FePO}_4$ and in Li_yFePO_4 (x, y small) excess charge carriers are created by Li^+ or their vacancies. It is expected that polarons and lithium ions are not diffusing independently due to lattice distortions and Coulomb interaction between them. A key value is the electrostatic binding or association energy between a positively (negatively) charged

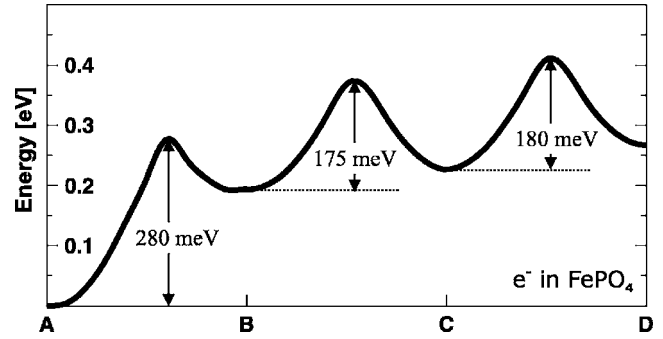


FIG. 4. Total energy along polaron migration path in $\text{Li}(\text{FePO}_4)_{64}$ along four adjacent iron sites from Fe_A to Fe_D ($U = 4.3$ eV). The distances between the Li^+ ion and the corresponding iron site are $r_A = 3.18$ Å, $r_B = 5.50$ Å, $r_C = 9.18$ Å, and $r_D = 12.72$ Å, respectively.

lithium ion (vacancy) and a negatively (positively) charged electron (hole) polaron. With the intention to limit finite size effects, that is to minimize the interaction of an isolated Li site with its mirror images across the boundary conditions, a supercell containing 64 formula units of FePO_4 containing one single lithium ion is investigated. Figure 4 shows the total energy along a migration path starting from an Fe site A, adjacent to a lithium ion, via two intermediate sites B and C to an Fe site D as far away from the Li^+ ion as possible in this cell. Along this path, the $\text{Li}^+ - \text{Fe}^{2+}$ distance increases from 3.18 Å to 12.72 Å. The activation barriers from A to B, B to C, and C to D are 280 meV, 175 meV, and 180 meV, respectively. The energy difference between the equilibrium sites A and B, B and C, and C and D are 200 meV, 35 meV, and 40 meV, respectively.

Due to the long range character of the electrostatic interaction, the Li^+ ion and electron in a supercell interact with mirror images across the periodic cell boundaries. By using an Ewald-type summation of the Coulomb potential proportional to $1/r$, the spurious interaction between the images of the Li^+ ion and the electron polaron can be subtracted leading to a value of 370 meV for the truly isolated configuration. A similar study for a single lithium vacancy and a hole polaron in LiFePO_4 reveals a binding energy larger than 500 meV, significantly higher than that for FePO_4 . The binding energy is much larger than typical exciton binding energies in semiconductors. This can be understood in terms of different electron localization in semiconductors and transition metal oxides: valence electrons in insulating transition metal oxides exhibit a much larger localization than those in semiconductors. Consequently, the screening, that is the damping of electric fields caused by the presence of mobile charge carriers, is much less pronounced in insulators than in semiconductors. Additionally, the binding energy is significantly higher than the corresponding activation barriers for *free* small polarons in both FePO_4 and LiFePO_4 . Hence, trapping of polarons by lithium ions or vacancies will be substantial and result in much lower electron conductivity than the activation barriers for *free* polarons suggest.

V. DISCUSSION

We have presented a GGA+ U approach in combination with a plane wave basis set to investigate small polaron mi-

gration in Li_xFePO_4 . Since our approach is not based on empirical models and does not incorporate assumptions specific to the olivine structure, it is generally applicable to polaron conducting systems. In order to evaluate the predictive quality of our method, we also investigated $\alpha\text{-Fe}_2\text{O}_3$ (hematite) which is known to be a small polaron conductor. Using a U value of 4 eV, we obtained 100 meV as the activation energy to free small polaron migration, which is in excellent agreement with the experimental evidence^{48,49} and other recent theoretical studies.^{25,28}

Moderately low activation barriers of 215 meV and 175 meV in LiFePO_4 and FePO_4 , respectively, are obtained for free polaron motion suggesting a high intrinsic electron mobility. However, our results also indicate a large binding energy between the charge carrier donor, that is the Li^+ ion or vacancy, making free polarons in the material unlikely. In Li_yFePO_4 , the binding energy between an electron and Li^+ ion is 370 meV. In $\text{Li}_{1-x}\text{FePO}_4$, the hole-vacancy binding energy is greater than 500 meV. Such a strong binding suggests that lithium ions and polarons may diffuse together as excitonlike quasiparticles through the crystal. One would expect that the activation energy of such ambipolar diffusion is significantly higher than those for free polaron and free lithium ion transfer. The strong coupling between electron (hole) polaron and Li^+ (vacancy) makes the interpretation of macroscopic transport more difficult. DC conductivity measurements with Li-blocking electrodes will likely be dominated by the Li^+ -polaron binding energy and may cause a Li^+ accumulation at the electrodes. In AC measurements, both Li^+ (vacancies) and polarons will move. The reorientation of bound dipoles (Li^+ -electron polaron or vacancy-hole polaron) will appear as a capacitive effect and solely their dissociation can lead to a current component in phase with the potential. Hence, we believe that conductivity measurements should be reinterpreted in the context of bound carriers. Our results indicate that, at least in the intrinsic material, the polarons strongly bind to the defect that creates them (Li^+ in FePO_4 or vacancies in LiFePO_4).

Our results leave open the question as to whether doping of LiFePO_4 can increase its electronic conductivity. In the

case where additional charge carriers are created by supervalent dopants, e.g., Mg^{2+} , Al^{3+} , Ti^{4+} , Zr^{4+} , Nb^{5+} , or W^{6+} substitute for Li^+ , charge neutrality would require a lithium deficiency in Li_xFePO_4 and could produce an excess of free, unbound lithium vacancies in LiFePO_4 or free, unbound electron polarons in FePO_4 .⁴ Correspondingly, subvalent doping on the Fe crystal sites could create an excess of free, unbound hole polarons in LiFePO_4 or free, unbound lithium ions in FePO_4 . Whether these doping-generated carriers would move with a lower activation barrier would depend on whether they are bound to their dopant ion or not. Given the strong binding between polaron and Li vacancies that we find, such binding seems very plausible, though a detailed computational analysis cannot be pursued without more information on the defect site and charge compensation mechanism.

Since the activation barrier to free motion as well as the Li^+ -polaron binding energy is lower in FePO_4 than in LiFePO_4 , we predict FePO_4 to be a better conductor than LiFePO_4 . This assumes that their levels of off-stoichiometry are similar. Such a difference of conductivity for LiFePO_4 and FePO_4 should become visible as hysteresis between charge and discharge of LiFePO_4 electrodes.

Electron transport and mixed ion-electron conduction in oxides is clearly of importance for many applications. Removal of the self-interaction from LDA/GGA with methods such as LDA/GGA+ U or other self-interaction correction (SIC) methods⁵⁰ create stable polarons and open up this important field for *ab initio* studies.

ACKNOWLEDGMENTS

The authors thank Dane Morgan and Anton Van der Ven for helpful discussions. This work was supported by the Department of Energy under Contract No. DE-FG02-96ER45571 and by the MRSEC program of the National Science Foundation under Contract No. DMR-0213282. Additional computing resources were provided by the National Science Foundation, National Partnership for Advanced Computing Infrastructure (NPACI).

*Email address: maxisch@mit.edu

†Email address: gceder@mit.edu; web: http://burgaz.mit.edu

¹A. K. Padhi, K. S. Nanjundaswamy, and J. B. Goodenough, *J. Electrochem. Soc.* **144**, 1188 (1997).

²A. K. Padhi, K. S. Nanjundaswamy, C. Masquelier, S. Okada, and J. B. Goodenough, *J. Electrochem. Soc.* **144**, 1609 (1997).

³H. Huang, S. C. Yin, and L. F. Nazar, *Electrochem. Solid-State Lett.* **4**, A170 (2001).

⁴S. Y. Chung, J. T. Bloking, and Y. M. Chiang, *Nat. Mater.* **1**, 123 (2002).

⁵C. Delacourt, L. Laffont, R. Bouchet, C. Wurm, J. B. Leriche, M. Morcrette, J. M. Tarascon, and C. Masquelier, *J. Electrochem. Soc.* **152**, A913 (2005).

⁶P. S. Herle, B. Ellis, N. Coombs, and L. F. Nazar, *Nat. Mater.* **3**, 147 (2004).

⁷D. Morgan, A. Van der Ven, and G. Ceder, *Electrochem. Solid-State Lett.* **7**, A30 (2004).

⁸M. Takahashi, S. Tobishima, K. Takei, and Y. Sakurai, *Solid State Ionics* **148**, 283 (2002).

⁹S. Q. Shi, L. J. Liu, C. Y. Ouyang, D. S. Wang, Z. X. Wang, L. Q. Chen, and X. J. Huang, *Phys. Rev. B* **68**, 195108 (2003).

¹⁰Y. N. Xu, S. Y. Chung, J. T. Bloking, Y. M. Chiang, and W. Y. Ching, *Electrochem. Solid-State Lett.* **7**, A131 (2004).

¹¹S. Y. Chung and Y. M. Chiang, *Electrochem. Solid-State Lett.* **6**, A278 (2003).

¹²N. Ravet, A. Abouimrane, and M. Armand, *Nat. Mater.* **2**, 702 (2003).

¹³R. A. Marcus, *Rev. Mod. Phys.* **65**, 599 (1993).

¹⁴K. V. Mikkelsen and M. A. Ratner, *Chem. Rev. (Washington, D.C.)* **87**, 113 (1987).

- ¹⁵N. Sutin, *Prog. Inorg. Chem.* **30**, 441 (1983).
- ¹⁶R. R. Dogonadze, A. M. Kuznetsov, and T. A. Marsagishvili, *Electrochim. Acta* **25**, 1 (1980).
- ¹⁷R. D. Cannon, *Electron Transfer Reactions* (Butterworths, London, 1980).
- ¹⁸A. S. Alexandrov and N. F. Mott, *Polarons & Bipolarons* (World Scientific, Singapore, 1995).
- ¹⁹S. R. Elliott, *The Physics and Chemistry of Solids* (Wiley, Chichester, 1998).
- ²⁰P. A. Cox, *The Electronic Structure and Chemistry of Solids* (Oxford University Press, Oxford, 1987).
- ²¹F. Zhou, C. A. Marianetti, M. Cococcioni, D. Morgan, and G. Ceder, *Phys. Rev. B* **69**, 201101(R) (2004).
- ²²C. Delacourt, P. Poizot, J. M. Tarascon, and C. Masquelier, *Nat. Mater.* **4**, 254 (2005).
- ²³V. Srinivasan and J. Newman, *J. Electrochem. Soc.* **151**, A1517 (2004).
- ²⁴A. Yamada, H. Koizumi, N. Sonoyama, and R. Kanno, *Electrochem. Solid-State Lett.* **8**, A409 (2005).
- ²⁵K. M. Rosso, D. M. A. Smith, and M. Dupuis, *J. Chem. Phys.* **118**, 6455 (2003).
- ²⁶A. Farazdel, M. Dupuis, E. Clementi, and A. Aviram, *J. Am. Chem. Soc.* **112**, 4206 (1990).
- ²⁷K. M. Rosso and M. Dupuis, *J. Chem. Phys.* **120**, 7050 (2004).
- ²⁸N. Iordanova, M. Dupuis, and K. M. Rosso, *J. Chem. Phys.* **122**, 144305 (2005).
- ²⁹R. A. Marcus, *Annu. Rev. Phys. Chem.* **15**, 155 (1964).
- ³⁰P. Tang and N. A. W. Holzwarth, *Phys. Rev. B* **68**, 165107 (2003).
- ³¹S. Shi, C. Ouyang, Z. Xiong, L. Liu, Z. Wang, H. Li, D. S. Wang, L. Chen, and X. Huang, *Phys. Rev. B* **71**, 144404 (2005).
- ³²A. Yamada, M. Hosoya, S. C. Chung, Y. Kudo, K. Hinokuma, K. Y. Liu, and Y. Nishi, *J. Power Sources* **119-121**, 232 (2003).
- ³³Y. N. Xu, W. Y. Ching, and Y. M. Chiang, *J. Appl. Phys.* **95**, 6583 (2004).
- ³⁴F. Zhou, K. Kang, T. Maxisch, G. Ceder, and D. Morgan, *Solid State Commun.* **132**, 181 (2004).
- ³⁵V. I. Anisimov, J. Zaanen, and O. K. Andersen, *Phys. Rev. B* **44**, 943 (1991); V. I. Anisimov, I. V. Solovyev, M. A. Korotin, M. T. Czyżyk, and G. A. Sawatzky, *Phys. Rev. B* **48**, 16929 (1993).
- ³⁶F. Zhou, M. Cococcioni, C. A. Marianetti, D. Morgan, and G. Ceder, *Phys. Rev. B* **70**, 235121 (2004).
- ³⁷F. Zhou, M. Cococcioni, K. Kang, and G. Ceder, *Electrochem. Commun.* **6**, 1144 (2004).
- ³⁸O. Le Bacq, A. Pasturel, and O. Bengone, *Phys. Rev. B* **69**, 245107 (2004).
- ³⁹O. Le Bacq and A. Pasturel, *Philos. Mag.* **85**, 1747 (2005).
- ⁴⁰M. Cococcioni and S. de Gironcoli, *Phys. Rev. B* **71**, 035105 (2005).
- ⁴¹A. I. Liechtenstein, V. I. Anisimov, and J. Zaanen, *Phys. Rev. B* **52**, R5467 (1995).
- ⁴²S. L. Dudarev, G. A. Botton, S. Y. Savrasov, C. J. Humphreys, and A. P. Sutton, *Phys. Rev. B* **57**, 1505 (1998).
- ⁴³J. P. Perdew, K. Burke, and M. Ernzerhof, *Phys. Rev. Lett.* **77**, 3865 (1996).
- ⁴⁴G. Kresse and J. Furthmüller, *Comput. Mater. Sci.* **6**, 15 (1996); G. Kresse and J. Furthmüller, *Phys. Rev. B* **54**, 11169 (1996).
- ⁴⁵J. Franck, *Trans. Faraday Soc.* **21**, 536 (1925); E. Condon, *Phys. Rev.* **28**, 1182 (1926); E. Condon, *Phys. Rev.* **32**, 858 (1928).
- ⁴⁶E. O. Wollan and W. C. Koehler, *Phys. Rev.* **100**, 545 (1955).
- ⁴⁷G. Rousse, *Chem. Mater.* **15**, 4082 (2003); R. P. Santoro and R. E. Newnham, *Acta Crystallogr.* **22**, 344 (1967).
- ⁴⁸J. B. Goodenough, in *Progress in Solid State Chemistry*, edited by H. Reiss (Pergamon, Oxford, 1971), Vol. 5, pp. 145–399.
- ⁴⁹E. Gharibi, A. Hbika, B. Dupré, and C. Gleitzer, *Eur. J. Solid State Inorg. Chem.* **27**, 647 (1990).
- ⁵⁰A. Zunger, J. P. Perdew, and G. L. Oliver, *Solid State Commun.* **34**, 933 (1980); J. P. Perdew and A. Zunger, *Phys. Rev. B* **23**, 5048 (1981).